

Effects of impurity location on the impurity bands and their spectral densities in quantum wells

A. Gold,* A. Ghazali, and J. Serre

*Groupe de Physique des Solides de l'Ecole Normale Supérieure, Université de Paris VII, tour 23, 2 place Jussieu,
F-75251 Paris CEDEX 05, France*

(Received 14 February 1989)

The electronic density of states and the spectral density of quantum wells are calculated as functions of the impurity position z_i . A multiple-scattering method which accounts for the formation of impurity bands is used. The study of the spectral densities provides us with the behavior of the averaged wave functions of the ground- and excited-state impurity bands in the \mathbf{k} space. We demonstrate that our approach can be used to study hybridization effects between different bands.

Shallow impurities in restricted geometries such as quantum wells have recently been studied both experimentally (for a review, see Ref. 1) and theoretically (for a review, see Ref. 2). The calculations of the bound states of Coulomb-like impurities are usually done in the single-impurity limit via variational methods³ and cannot account for the overlap of impurity wave functions.

Recently, we have calculated impurity bands in silicon metal-oxide-semiconductor structures⁴ and in quantum wells.⁵ We have studied impurity bands well separated from the conduction band (at low impurity concentration N_i) and band tails (at high impurity concentration). The merging of excited impurity bands for impurities located at the center of the well has been discussed in Ref. 6. There we have also studied the spectral density which is connected to the configuration-averaged wave functions in the \mathbf{k} space. We were able to describe hybridization effects when the impurity bands come near each other.

The aim of this paper is to investigate the effects of the location z_i of impurities on the electronic structure of ground- and excited-state impurity bands and of the conduction-band edge. Our numerical results apply to the case of a GaAs quantum well. Specifically, we study the energy location of the band edges and the evolution of the spectral density (SD) and the density of states (DOS) as functions of z_i . The merging of the impurity bands (IB's) which yields a band tail by varying z_i is also studied. As N_i goes to zero we find that the energy of the ground- and the excited-state IB's is in agreement with the variational results.^{2,7} As we have shown recently, the SD analysis allows one to clearly distinguish between $1s$ and $2p_{\pm}$ states for impurities located at the center of the quantum well.⁶ A change from the $1s$ to the $2p_0$ symmetry of the ground state as a function of the location z_i of impurities has been shown by Lane and Greene;⁷ this point will be discussed below.

As in Refs. 4–6 we calculate the one-electron Green's function $G(\mathbf{k}, E)$ for the vector \mathbf{k} and energy E for a two-dimensional electron gas in the presence of charged impurities. The imaginary part of the Green's function defines the spectral density $A(\mathbf{k}, E)$. The density of states is calculated as the sum of $A(\mathbf{k}, E)$ over the \mathbf{k} 's and

the spin states. The self-energy in the Green's function which is due to charged impurity scattering is calculated with Klauder's best multiple-scattering method.⁸ For details, see Ref. 4.

Two infinite potential barriers in the x - y plane at $z=0$ and $z=L$ define the quantum well (QW) with width L . Impurities are randomly distributed in the x - y plane at a distance z_i from the left interface. $z_i=0$ and $z_i=L/2$ correspond to impurities located on the edge and at the center of the QW, respectively. The screened electron-impurity interaction formula was given in Ref. 6. For the form factors which enter the expressions of the bare electron-impurity interaction and the screening function we use results given in Ref. 9. The form factors account for the finite width of the QW and also for the impurity position z_i .

In the inset of Fig. 1 we show the DOS versus energy for a QW with $L=100$ Å, electron density $N=1 \times 10^8$ cm⁻², impurity density $N_i=1 \times 10^8$ cm⁻², and $z_i=L/2$. The units of the DOS and of the energy are the free-electron DOS and the effective Rydberg, respectively. The screening effect reduces the binding energy of shallow impurities.¹⁰ Experimental results¹ indicate that impurities in QW's are slightly screened. Our systematic study of the binding energy versus electron density⁵ confirms this result: for $N < 1 \times 10^8$ cm⁻² the binding energy is nearly independent on N and this indicates that for $N < 1 \times 10^8$ cm⁻² we are dealing with nearly unscreened impurities.

With parameters used in the inset of Fig. 1 we found three IB's. The energies of the edges of these bands, as indicated in the inset of Fig. 1, versus z_i are shown in Fig. 1. The strong z_i dependence of the binding energy of the ground-state IB contrasts with the weaker one of the excited-state IB's. This is in agreement with the variational results.⁷ The high- (low-) lying excited IB merges with the conduction band (CB) at $z_i = -0.2L$ ($-0.9L$), respectively. Clearly, these values depend on N , N_i , and L . In realistic systems the barrier height of QW is finite. In this situation, the wave function extends outside the well. It is then expected that the electron-impurity interaction is weaker when the impurities are located inside

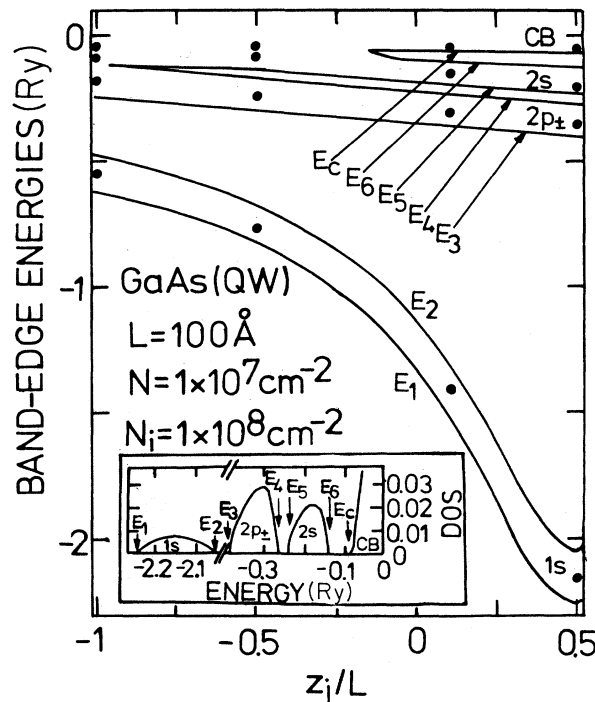


FIG. 1. Band-edge energies (see inset) vs the location for impurities z_i . The inset shows a typical DOS vs energy for impurities located in the center of the QW. The dots indicate the z_i and energy values for which we show the spectral density, see Fig. 2. Ry is the effective Rydberg.

the well and stronger when they are outside, because of evident electron-impurity proximity effects. The width W of the IB's increases with increasing impurity density, $W \propto N_i^{1/2}$, as found in the coherent-potential approximation for a different system.¹¹ The merging of an IB with the CB can arise either from an increase of N_i (Refs. 4-6) or from an increase of $|z_i|$. The latter effect is demonstrated in Fig. 1.

More information on the nature of the IB's is contained in the SD, which is given by $A(\mathbf{k}, E) = -(1/\pi)\text{Im}G(\mathbf{k}, E + i0)$. One can show (see Ref. 6 and Ref. 16 therein) that

$$A(\mathbf{k}, E) = \frac{1}{\Omega} \left\langle \sum_j |\Psi_j(\mathbf{k})|^2 \delta(E - E_j) \right\rangle. \quad (1)$$

$\Psi_j(\mathbf{k})$ is the Fourier transform of the wave function $\Psi_j(\mathbf{r})$. $\langle \dots \rangle$ represents the impurity-configuration average and the sum runs over the eigenstates. Ω is the area. For $N_i \rightarrow 0$, we get

$$A(\mathbf{k}, E) = N_i g_j |\Psi_j(\mathbf{k})|^2 \delta(E - E_j). \quad (2)$$

Here, g_j is the degeneracy of the atomic state with the eigenenergy $E = E_j$ and the SD is determined by the wave functions of the single impurity problem. In Ref. 6 we have calculated the Fourier transform of the wave functions ($1s, 2s, 2p_{\pm}, 3s, 3p_{\pm}, 3d_{\pm}$) for the ideally two-dimensional Coulomb problem ($L=0, z_i=0$) (Ref. 12) and found an excellent agreement with our numerical results for $A(\mathbf{k}, E)$ at low N_i , according to Eq. (2). It is

worth noticing that the squared Fourier transform $|\psi(k)|^2$ for a pure $2p_{\pm}$ state behaves as k^2 for $k \rightarrow 0$ (Ref. 6), while for $1s$ and $2s$ states it has the form $\alpha - \beta k^2$, where α and β are positive constants. Thus, for $z_i=0$, we have identified the IB's as $1s, 2p_{\pm}$, and $2s$ IB's with the same energy ordering as found with variational calculations,^{2,7} see inset of Fig. 1. Let us remark that we found a twofold degeneracy for the $2p_{\pm}$ IB as expected.

In Fig. 2, we show the SD versus the wave number for the same parameters (L, N, N_i) as in Fig. 1. The solid, dashed, dashed-dotted, and dotted lines are for $z_i=50, 10, -50$, and -100 Å, respectively. The corresponding energy values are indicated in Fig. 1 as solid circles. As the impurities are moved away from the center of the QW, the IB wave functions become more localized in the two-dimensional \mathbf{k} space [see Eq. (2) and Fig. 2], i.e., more extended in the x - y plane. This effect is stronger for the ground state than for the excited states and reflects

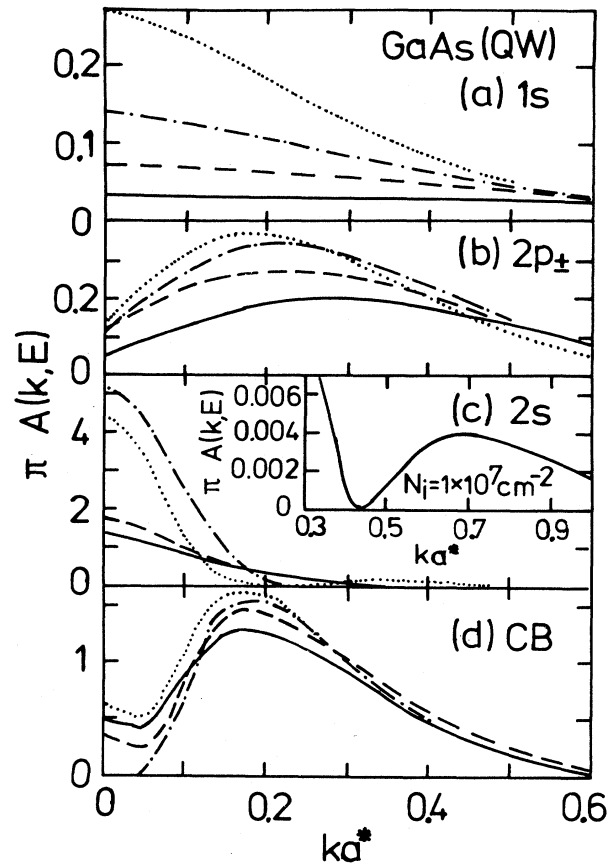


FIG. 2. Spectral density $A(k, E)$ vs wave number k for (a) the ground-state IB, (b) the first low-lying excited-state IB, (c) the next-low-lying excited state IB, and (d) states near the CB edge. Solid, dashed, dashed-dotted, and dotted lines are for $z_i=50, 10, -50$, and -100 Å, respectively. The energy values are indicated in Fig. 1. For L, N_i , and N we used the same values as in Fig. 1. The inset shows the spectral density at the center of the well for the $2s$ state for $N_i=1 \times 10^7 \text{ cm}^{-2}$ and for larger wave numbers. a^* is the Bohr radius.

the z_i dependence of their respective binding energies.

Lane and Greene⁷ have shown that as a single impurity is moved from the center to the edge of a QW, the ground state undergoes a symmetry change from $1s$ to $2p_0$ state while the $2p_{\pm}$ excited states take the character $3d_{\pm}$. A ground state of $2p_0$ symmetry is found in the case of an impurity located at the interface with infinite barrier height, the electron moving in the semiconductor half-space. This is what we refer to hereafter as Levine's geometry.¹³

Now, in Fig. 2(a), as the impurities are moved from the center, the shape of the SD remains qualitatively unchanged in the sense that it has the form $\alpha\beta k^2$ for small k ; however, α increases. Let us first remark that the QW width we have considered with impurities located on the QW edge corresponds to a situation intermediate between the ideally two-dimensional system and the Levine's geometry. To get a better understanding of this situation we have done the following. (i) We have calculated analytically the SD for a single impurity according to Eq. (2) in the Levine's geometry.¹³ We found indeed that $A(\mathbf{k}, E) \sim \alpha - \beta k^2$ as $k \rightarrow 0$, the constant α being much larger than that of the $1s$ ground state in two dimensions.⁶ (ii) We have simulated the change from the pure two-dimensional geometry to Levine's one by increasing the QW width from 100 to 800 Å and by putting the impurities on the QW edge. Using our multiple-scattering method, we get the SD. In all cases studied, we obtained for the ground-state IB a SD of the form $\alpha\beta k^2$ (as $k \rightarrow 0$), α being larger as the QW becomes wider. This is in agreement with the expected gradual change from the $1s$ to $2p_0$ -ground-state IB, as one goes from one geometry to the other. All these results confirm the work of Lane and Greene.⁷

The wave function of a $2p_{\pm}$ state has a maximum at finite k , see Fig. 2(b) and Ref. 6. The finite value of $A(\mathbf{k} \rightarrow 0, E)$ for the $2p_{\pm}$ in Fig. 2 is due to the hybridization effects between the $2p_{\pm}$ IB and the $2s$ IB; see also Ref. 6, where hybridization effects versus N_i are discussed.

The Fourier transform of the wave function of the $2s$ state has a node at a finite wave number. For the ideally two-dimensional Coulomb problem the node occurs at $ka^* = \frac{2}{3}$.⁶ a^* is the Bohr radius. Due to the finite width of the QW this number is reduced (the wave function is more delocalized in the x - y plane) and the node occurs at

$ka^* \approx 0.45$; see the inset in Fig. 2(c), where we have shown the SD for a lower density ($N_i = 1 \times 10^7 \text{ cm}^{-2}$) in order to reduce hybridization effects.

The SD near the CB edge, see Fig. 2(d), is probably reminiscent of the $3s$, $3p_{\pm}$, and $3d_{\pm}$ atomic states. The strong energy dependence of the SD (Ref. 6) near the CB edge complicates the interpretation of the SD versus z_i in terms of single-atomic orbitals. The broad minimum indicates that the main contribution to the SD comes from the $3d_{\pm}$ states, where $|\Psi(k)|^2$ is proportional to k^4 as $k \rightarrow 0$ and shows a maximum at $k \approx 0.25$.⁶

To explain how the above hybridization effects are included in our multiple-scattering method, let us recall that this method is an alternative way to solve the many-impurity quantum problem. Starting with an unperturbed system, the multiple-scattering equation is the result of the summation of a series expansion in powers of concentrations and potentials.¹⁴ It is then not surprising that as soon as the IB's come near each other, a mixing of the corresponding states occurs due to the perturbing potential.

To summarize, we have calculated the dependence of the binding energy and of the width of IB's ($1s, 2p_{\pm}, 2s$) in QW's on the impurity position z_i . The binding energy is in good agreement with variational results.^{2,7} Even for a rather low impurity concentration $N_i = 1 \times 10^8 \text{ cm}^{-2}$ the calculated width of the IB's indicates that the overlap of the impurity wave functions cannot be neglected and it is indeed important for a consistent interpretation of experiments.¹

The study of the spectral density in the limit of low impurity density gives evidence that the ground-state IB has an s character for impurities located at the center of the QW. A gradual mixing with the $2p_0$ character is observed as the impurities are moved towards the QW edge, in agreement with the results of Ref. 7. We have shown that hybridization effects between the different atomiclike levels can be studied within our theory.

A. Gold thanks the Deutsche Forschungsgemeinschaft (Bonn, Germany) for financial support. The Groupe de Physique des Solides de l'Ecole Normale Supérieure is a Laboratoire associé au Centre National de la Recherche Scientifique (France).

*Present address: Department of Physics, Massachusetts Institute of Technology, Cambridge, Massachusetts 02139.

¹B. V. Shanabrook, *Physica B+C* **146B**, 121 (1987).

²Y.-C. Chang, *J. Phys. (Paris) Colloq.* **48**, C5-375 (1987); G. Bastard, *Wave Mechanics Applied to Semiconductor Heterostructures* (Editions de Physique, Les Ullis, 1988).

³G. Bastard, *Phys. Rev. B* **24**, 4714 (1981).

⁴A. Gold, J. Serre, and A. Ghazali, *Phys. Rev. B* **37**, 4589 (1988); A. Ghazali, A. Gold, and J. Serre, *Surf. Sci.* **196**, 346 (1988).

⁵J. Serre, A. Ghazali, and A. Gold, *Phys. Rev. B* **39**, 8499 (1989); A. Gold, J. Serre, and A. Ghazali, in *19th International Conference on the Physics of Semiconductors*, edited by W. Zawadzki (Institute of Physics, Polish Academy of Sciences, Warsaw, 1988), p. 299.

⁶A. Ghazali, A. Gold, and J. Serre, *Phys. Rev. B* **39**, 3400 (1989).

⁷P. Lane and R. L. Greene, *Phys. Rev. B* **33**, 5871 (1986).

⁸J. R. Klauder, *Ann. Phys. (N.Y.)* **14**, 43 (1961).

⁹A. Gold, *Phys. Rev. B* **35**, 723 (1987).

- ¹⁰J. A. Brum, G. Bastard, and C. Guillemot, *Phys. Rev. B* **30**, 905 (1984).
- ¹¹H. Ehrenreich and L. M. Schwartz, in *Solid State Physics*, edited by F. Seitz, D. Turnbull, and H. Ehrenreich (Academic, New York, 1976), Vol. 31, Sec. IV, p. 149.
- ¹²S. Flügge and H. Marshall, *Rechenmethoden der Quantentheorie*, 2nd ed. (Springer, Berlin, 1952), Problem 24; B. Zaslów and M. E. Zandler, *Am. J. Phys.* **35**, 1118 (1967).
- ¹³J. D. Levine, *Phys. Rev.* **140**, A586 (1965).
- ¹⁴J. Serre and A. Ghazali, *Phys. Rev. B* **28**, 4704 (1983), Appendix A.